Determination of two-dimensional current patterns in flat superconductors from magneto-optical measurements: An efficient inversion scheme

Rinke J. Wijngaarden, H. J. W. Spoelder, R. Surdeanu, and R. Griessen
Institute COMPAS and Department of Physics and Astronomy, Vrije Universiteit, De Boelelaan 1081, 1081 HV Amsterdam, The Netherlands
(Received 11 March 1996)

An efficient inversion scheme is given to derive the local currents in a superconductor from the z component of the magnetic field measured above its surface, as is done using magneto-optical indicators. The method works for samples of arbitrary thickness provided that the current vector has only x and y components. Data storage is much lower and convergence much faster than in previously reported schemes. The influence of the distance of observation and of the sample aspect ratio on the measured field H_z is investigated. The current calculated from the magneto-optical observation of a real sample (a $Bi_2Sr_2CaCu_2O_8$ single crystal) is in good agreement with the value measured directly by means of torque magnetometry. [S0163-1829(96)07534-0]

I. INTRODUCTION

The current distribution in type-II superconductors of various shapes in a magnetic field has been the subject of many theoretical papers. For example the shielding currents for the strip geometry were considered by Brandt *et al.*[1] and for a disk by Frankel[2] and Brandt[3] while also Zeldov *et al.*[4] considered this problem. The flux penetration process was considered by Fedorov *et al.*[5] and for rectangular samples by Brandt.[6]

Magneto-optical observations of superconductors give detailed information on the z component of the local magnetic field and for this reason the magneto-optical technique has become increasingly popular (the z component is defined by the normal to the plane of the magneto-optical detector). It is not widely realized that the magneto-optical technique can also yield accurate values for the local current densities and for their relaxation in time. An attempt to determine the currents in a disk-shaped sample from magneto-optical observations was made by Theuss *et al.*,[7] who used adjustable currents through a set of concentric conducting rings to fit calculated H_z values to measured ones. Clearly, in this case the geometry of the current pattern is fixed from the outset. This is a severe disadvantage, e.g., for samples with unknown defects.[8] A method which finds not only the currents, but also the current flow pattern is given by Brandt,[9] while a similar method was later given by Xing *et al.*[10] Both methods work for infinitely thin samples only and the absolute calibration of the currents is difficult due to the fast change with distance of the magnetic field above such samples and the fact that in real measurements this distance is not known precisely. In the present paper this problem is solved by taking the thickness of the samples explicitly into account. We consider a sample which is a rectangular cylinder of arbitrary cross section and arbitrary height (see Fig. 1) which we will designate for simplicity henceforth as a ''flat'' sample. In the next section a relation between the currents in such a sample and the z component of the magnetic field, H_z, is derived. In Sec. III this relation is numerically inverted by making use of the fact that H_z is measured at discrete positions. In Sec. IV we show that the currents in the sample can be found even if the distance between the detector and the sample is not known accurately. In Sec. V our formalism is applied to measurements on a real sample (a $Bi_2Sr_2CaCu_2O_8$ single crystal) and the results are compared to macroscopic measurements of the current.

II. FINDING THE CURRENTS FROM THE FIELD H_z: ANALYTICAL FORMALISM

In a typical magneto-optical experiment, shown schematically in Fig. 1 and to be discussed in more detail in Sec. III, the z component of the magnetic field, H_z^{meas} is measured at a distance d above a superconducting sample. The purpose of this paper is to find the currents flowing in the sample from the measured $H_z^{\mathrm{meas}}(x,y,d)$ values. If the measurements are performed in an external field H_z^{ext} then

$$\vec{H}^{\mathrm{meas}}=\vec{H}^{\mathrm{ext}}+\vec{H}^{\mathrm{self}}, \tag{1}$$

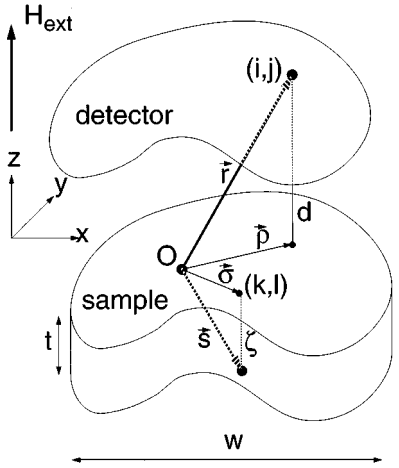

FIG. 1. Schematic representation of the measurement layout. The detector plane indicates the position of the magneto-optical layer. The distances and vectors are explained in the text.

where the self-field $\vec{H}^{\rm self}$ is the field generated by the currents in the sample. In an experiment the external field component $H_z^{\rm ext}$ is known, $H_z^{\rm meas}$, is measured, and the z component of the self-field, $H_z^{\rm self}$, can thus be found using Eq. (1).

To derive an algorithm for the calculation of the currents in the sample from $H_z^{\rm self}$, we first prove in this section that any two-dimensional (2D) current flow can be decomposed into a spatial distribution of magnetic dipole moments of unit strength. For simplicity of notation the self-field will from now on be designated by $\vec{H}$ in this and in the next section. The self-field $\vec{H}$ at any position $\vec{r}$ induced by an electrical current density $\vec{j}(\vec{s})$ in the sample is given by the Biot-Savart formula[11]

$$\vec{H}(\vec{r})=\frac{1}{4\pi}\int_V \vec{j}(\vec{s})\times\frac{\vec{r}-\vec{s}}{|\vec{r}-\vec{s}|^3}d^3s, \tag{2}$$

where the integral is over the volume of the sample V. Since there are no currents flowing outside the sample, the integral can of course also be taken over the whole space. For a 2D current pattern, where the currents are flowing only in the x and y directions, Brandt[9] introduced the scalar field g, defined by

$$\vec{j}(\vec{s})\equiv\nabla_{\vec{s}}\times[g(\vec{s})\hat{z}]. \tag{3}$$

The definition in Eq. (3) guarantees that $\nabla\cdot\vec{j}=0$. In fact, g is defined apart from an integration constant and a gradient term, which both are chosen to be zero. It is important to note that contrary to Brandt[9] we do not use the concept of sheet currents; hence in the present work the dimension of g is $[A/m]$ and in Eq. (2) the current density is also integrated over the thickness of the sample. With the notation $\vec{m}\equiv g(\vec{s})\hat{z}$, substitution of Eq. (3) in Eq. (2) yields

$$\begin{aligned}\vec{H}(\vec{r})&=\frac{-1}{4\pi}\int_V\frac{\vec{r}-\vec{s}}{|\vec{r}-\vec{s}|^3}\times(\nabla_{\vec{s}}\times\vec{m})d^3s\\&\equiv\frac{-1}{4\pi}\int_V\vec{\Re}\times(\nabla_{\vec{s}}\times\vec{m})d^3s.\end{aligned} \tag{4}$$

The second equality defines the vector $\vec{\Re}$, which is used to simplify the notation. We now use the vector identity

$$\begin{aligned}\nabla_{\vec{s}}(\vec{m}\cdot\vec{\Re})=(\vec{m}\cdot\nabla_{\vec{s}})\vec{\Re}+(\vec{\Re}\cdot\nabla_{\vec{s}})\vec{m}+\vec{m}\times(\nabla_{\vec{s}}\times\vec{\Re})\\+\vec{\Re}\times(\nabla_{\vec{s}}\times\vec{m})\end{aligned} \tag{5}$$

and note that

$$\int_V\nabla_{\vec{s}}(\vec{m}\cdot\vec{\Re})d^3s=\int_S(\vec{m}\cdot\vec{\Re})\vec{n}d^2s=\vec{0}, \tag{6}$$

since $\vec{m}$ is zero outside the sample. In addition, using partial integration, we find

$$\int_V(\vec{\Re}\cdot\nabla_{\vec{s}})\vec{m}d^3s=-\int_V\vec{m}(\nabla_{\vec{s}}\cdot\vec{\Re})d^3s=\vec{0}, \tag{7}$$

since $\nabla_{\vec{s}}\cdot\vec{\Re}=0$, as can be easily verified. For the calculation of the field at positions $\vec{r}$ outside the sample, the partial integration is always justified because the numerator in $\vec{\Re}$ is always positive: $\vec{r}$ is always larger than $\vec{s}$ if $\vec{s}$ is inside the sample. From explicit calculation one finds

$$\nabla_{\vec{s}}\times\vec{\Re}=\vec{0}. \tag{8}$$

Substitution of Eq. (6)–(8) into Eq. (5) gives

$$\int_V\vec{\Re}\times(\nabla_{\vec{s}}\times\vec{m})d^3s=\int_V-(\vec{m}\cdot\nabla_{\vec{s}})\vec{\Re}d^3s, \tag{9}$$

and using the definition of $\vec{\Re}$ this may be further evaluated:

$$(\vec{m}\cdot\nabla_{\vec{s}})\vec{\Re}=\frac{1}{|\vec{r}-\vec{s}|^3}(\vec{m}\cdot\nabla_{\vec{s}})(\vec{r}-\vec{s})+(\vec{r}-\vec{s})(\vec{m}\cdot\nabla_{\vec{s}})\frac{1}{|\vec{r}-\vec{s}|^3}\cdot \tag{10}$$

From the fact that $\vec{m}$ has only a nonzero z component it follows that

$$(\vec{m}\cdot\nabla_{\vec{s}})(\vec{r}-\vec{s})=g(\vec{s})\hat{z}\frac{\partial}{\partial z}(r_z-z)=-\vec{m}. \tag{11}$$

Substitution in Eq. (10), carrying out the differentiation of $1/|\vec{r}-\vec{s}|^3$, and substitution of the result in Eq. (9) gives an expression for $\int_V\vec{\Re}\times(\nabla_{\vec{s}}\times\vec{m})d^3s$. If this is substituted in Eq. (4), one finds

$$\begin{aligned}\vec{H}(\vec{r})&=\frac{1}{4\pi}\int\frac{3\hat{n}(\vec{m}\cdot\hat{n})-\vec{m}}{|\vec{r}-\vec{s}|^3}d^3s\\&=\frac{1}{4\pi}\int g(\vec{s})\frac{3\hat{n}(\hat{z}\cdot\hat{n})-\hat{z}}{|\vec{r}-\vec{s}|^3}d^3s\end{aligned} \tag{12}$$

[with $\hat{n}=(\vec{r}-\vec{s})/|\vec{r}-\vec{s}|$]. This expression gives the field outside the sample for any 2D current flow $\vec{j}(\vec{s})=\nabla_{\vec{s}}\times\vec{m}$ with $\vec{m}=g(\vec{s})\hat{z}$.

It is easily verified that for $g(\vec{s})\hat{z}=\vec{\mu}\delta_3(\vec{s})$, Eq. (3) yields the current for the ideal dipole moment at the origin. If $\vec{m}=\vec{\mu}\delta_3(\vec{s})$ is substituted in Eq. (12), then it reduces to the well known[12] formula for the field of a dipole moment $\vec{\mu}$:

$$\vec{H}(\vec{r})=\frac{1}{4\pi}\frac{3\hat{r}(\vec{\mu}\cdot\hat{r})-\vec{\mu}}{r^3}, \tag{13}$$

where $\hat{r}=\vec{r}/|\vec{r}|$. This implies that the H_z field of any 2D current distribution $\vec{j}(\vec{s})$ can be expressed in terms of a spatial distribution $g(\vec{s})$ of magnetic dipole moments of unit strength, the relation between $\vec{j}(\vec{s})$ and $g(\vec{s})$ being given by Eq. (3).

To proceed with the calculation for this 2D current pattern we replace the vector $\vec{s}$ by the vector $(\vec{\sigma},\zeta)$, where ζ is the depth in the sample measured from the top surface; see Fig. 1. Likewise we replace the vector $\vec{r}$ by $(\vec{\rho},d)$ where d is the height above the sample where the magnetic field is measured. To be able to find the inversion scheme for calculating the current flowing in the sample from the measured external

field, one extra assumption is necessary. We take (within the sample) a current which is uniform over the thickness: $\vec{j}$ is independent of ζ, which through Eq. (3) also implies that g is independent of ζ.

Using this and the new variables, one obtains for samples of *any* thickness t from Eq. (12)

$$H_z(\vec{\rho},d)=\frac{1}{4\pi}\int_S g(\vec{\sigma})\int_0^t \frac{2(d+\zeta)^2-|\vec{\rho}-\vec{\sigma}|^2}{[|\vec{\rho}-\vec{\sigma}|^2+(d+\zeta)^2]^{5/2}}d\zeta d^2\sigma, \tag{14}$$

where the first integral is over any area containing the sample surface S [since $g(\vec{\sigma})$ is zero outside the sample]. It is this result which is at the basis of the inversion scheme discussed in the next section.

The assumption $g(\vec{\sigma},\zeta)=g(\vec{\sigma})$ (equivalent to a current which is uniform over the thickness of the sample) is justified for samples which are thin compared to the superconducting penetration depth λ, i.e., $t\leqslant\lambda$, because in a superconductor the current cannot vary over a scale smaller than λ. It is also justified (except, possibly, close to the upper and lower surfaces) in the other extreme case, a very long sample with $t\gg w$, because in this case there is translational symmetry along z. In the intermediate case $\lambda<t<w$ the situation is more complicated and may lead to a z-dependent current which is, however, still 2D. For $z>t$ it turns out that this is not really a problem.

A potential problem is the very strong pinning of vortices in which case the vortices may not be able to adjust their curvature (or density) to a changing external field. In such a case the current can be nonuniform over the thickness of the sample. For most superconductors this situation does not occur. In particular even at zero temperature high-T_c superconductors exhibit quantum creep,[13] which allows the vortices to relax; for these materials we thus expect a current uniform over the thickness. For further details the reader is referred to the discussion by Brandt.[14]

We note that for the case of straight vortices only (large sample thickness t), the local vortex density is proportional to $g(\vec{\sigma})$. In Sec. III a method is derived to find $g(\vec{\sigma})$ from $H_z(\vec{\rho},d)$; hence for straight vortices the magneto-optical measurement can be used to determine the vortex density directly.

In this section a method was derived to calculate $H_z(\vec{\rho},z)$ from $\vec{j}(\vec{\sigma})$ for flat samples of arbitrary thickness; in the next section we show that our goal of deriving $\vec{j}(\vec{\sigma})$ from the measured $H_z(\vec{\rho},z)$ values can be reached by discretizing the spatial variables.

III. FINDING THE CURRENTS FROM THE FIELD H_z: NUMERICAL INVERSION SCHEME

In a typical magneto-optical experiment, the z component of the magnetic field, H_z, above a sample is made visible by means of a magneto-optic (MO) layer parallel to the XY plane. Such a layer is usually made of materials with a large Faraday effect, such as EuS, EuSe, EuTe, and iron garnet films.[15] Between this layer and the sample top surface, a mirror layer is placed. Polarized light reflected by such a double layer has a polarization vector turned by an angle proportional to the z component of the local magnetic field in the layer. After having passed through an analyzer in crossed position with respect to the polarizer, the intensity of the reflected light is given by

$$I=I_0\sin^2(\gamma H_z), \tag{15}$$

where γ is the product of the thickness of the MO layer and its Verdet constant.[15] The experiment can be done in an imaging mode such that after the analyzer an image of the MO layer is formed on the charge-coupled-device (CCD) chip of a TV camera. From the intensity values measured by the CCD camera $|H_z|$ as a function of position on the sample can be obtained by means of Eq. (15). The sign of H_z is usually known from the history of the experiment, but can always be determined experimentally (if necessary) by turning one of the polarizers.[16]

To be able to derive an efficient inversion scheme [based on Eq. (14)] for the currents in a flat sample from the magneto-optical data, we discretize the measured $H_z(x,y,d)$ values. This is a natural procedure since, due to the construction of CCD cameras, the measured image is inherently discretized to, e.g., 768×576 so-called pixels. By image-processing techniques (binning) this number can be reduced. The number of significant pixels depends very much on the experiment. For simple current patterns 60×60 pixels may be sufficient, while for very complicated current patterns a maximum resolution of, e.g., 768×576 may be required.

To proceed, we identify the pixels along x and y by (i,j) in the detector. In analogy we also discretize the $g(\vec{\sigma})$ function and designate the pixels in the sample by (k,l) (see Fig. 1). The linear pixel size in the detector and sample, both along x and y, is set equal to a (square pixels). In Eq. 14, the integration along x and y is written explicitly by replacing $d^2\sigma$ by $d\eta d\xi$, while the integral over the sample is replaced by a sum over all pixels times an integral over a given pixel (and the sample thickness) to obtain

$$\begin{aligned}H_z(i,j,d)&=\frac{1}{4\pi}\sum_{k,l} g(k,l)\int_{k-1/2}^{k+1/2}\int_{l-1/2}^{l+1/2}\int_0^t \\ &\times\frac{2(d+\zeta)^2-a^2(\xi-i)^2-a^2(\eta-j)^2}{[(d+\zeta)^2+a^2(\xi-i)^2+a^2(\eta-j)^2]^{5/2}}d\zeta d\eta d\xi.\end{aligned} \tag{16}$$

The $g(k,l)$ is taken to be constant within one pixel (i.e., details in the current distribution can be seen down to the scale of one pixel, but finer details are lost) and hence is put in front of the integral. In this case the integral can be carried out easily using

$$\int\int\int \frac{2z^2-x^2-y^2}{[z^2+x^2+y^2]^{5/2}}dzdydx=-\arctan\frac{xy}{z\sqrt{x^2+y^2+z^2}}+C, \tag{17}$$

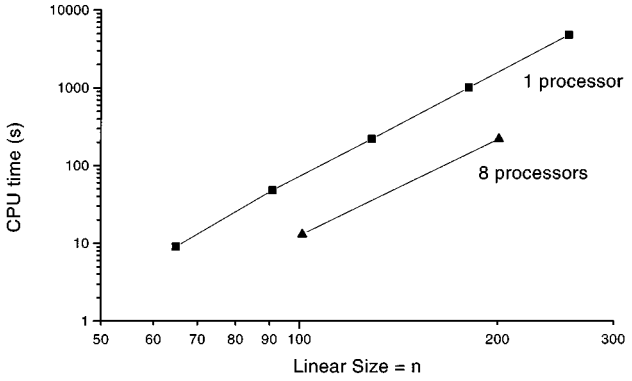

FIG. 2. Computer time (in CPU seconds) needed on a single processor or eight processors of an IBM SP2/9076 machine for the inversion of the matrix equation (18) for square images as a function of the linear size of the image.

where C is an integration constant. The analytical result is used in the computer programs to be discussed below. Since the value of the integral depends only on the distance d and the pixel size a, it is fixed once and for all for a given sample-detector configuration. For fixed a and d, it can be denoted by $M(i,j,k,l)$, whence Eq. (16) may be written as

$$H_z(i,j)=\frac{1}{4\pi}\sum_{k,l} M(i,j,k,l)g(k,l). \tag{18}$$

This is a matrix equation of the form $\mathbf{h}=\mathbf{Mg}$ from which $\mathbf{g}$ must be calculated: The currents in the sample can then be found from $\mathbf{g}$ using Eq. (3). Our problem is thus formally solved except for the inversion of the matrix equation (18).

In his 1992 paper,[9] by a clever use of physical knowledge of the problem, Brandt finds an iteration procedure which yields $\mathbf{g}$. Xing *et al.*[10] either invert $\mathbf{M}$ explicitly or use an *ad-hoc* procedure[17] for solving Eq. (18). In this iterative procedure $g(k,l)$ is continuously adjusted until Eq. (18) yields the measured $H_z(i,j)$. For the adjustment of $g(k,l)$, it is assumed that to first order an error in H_z at the point (i,j) can be corrected by adjusting $g(i,j)$ only. This method works, but is rather slow. A serious problem for the application to real experiments is that in all these methods the sample thickness is not taken into account. Due to this, the calculated currents depend very much on the assumed effective sample-detector distance d, which is not precisely known.

By contrast to these methods, our algorithm explicitly takes the sample thickness t into account and thereby (as will be shown below in Sec. IV) solves the problem of unknown distance between sample and detector. Also our method is more efficient due to the use of the conjugate gradient method in the iteration procedure and due to our observation that the matrix $\mathbf{M}$ is in fact a Toeplitz block Toeplitz matrix. This implies that very efficient storage is possible. If the image contains n^2 pixels, then $\mathbf{M}$ has n^4 elements. However, there are only n^2 *different* elements. If this fact is used, $\mathbf{M}$ requires not more storage space than the original image $H_z(k,l)$. Since it is not practical to invert $\mathbf{M}$ because it requires too much memory (e.g., for a 300×300 image 1.6×10^{10} bytes are needed), Eq. (18) is solved iteratively,

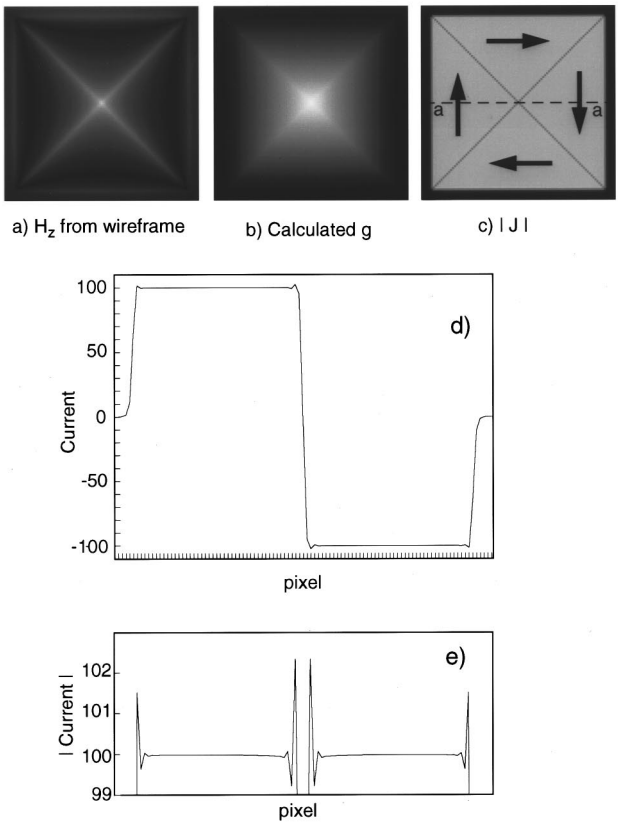

FIG. 3. Verification of the numerical algorithm on a 101×101 image. (a) H_z generated by a set of equidistant wires, each carrying the same current $j=100$, (b) g image as found from solving Eq. (18), (c) the absolute value of the calculated current (the arrows indicate the current flow direction), (d) cross section of (c) (but including the sign of the current) along the line a-a through the center and parallel to a side, showing that the calculated current matches very well the input current j in the wires, and (e) enlargement of (d) showing that the maximum error in the current amplitude $|j|$ is about 2% and occurs at the edge only. The dip in the center is caused by the change of flow direction.

using a standard conjugate gradient (CG) method. This method is applicable because $\mathbf{M}$ is a symmetric semipositive definite matrix. Compared to the *ad-hoc* method of Xing *et al.*,[17] it decreases the number of iteration steps by at least a factor of 5. No difference was found between the Fletcher-Reeves and Polak-Ribiere CG algorithms, indicating that the problem is well behaved (locally quadratic). In our algorithm, the number of iteration steps depends only weakly on the size of the image and the CPU time needed for the computation was found to scale as $n^{4.5}$; see Fig. 2. The calculations were done on an IBM SP2/9076 machine, which using a single processor needed 35 s for a size of 65×65 pixels (see Fig. 2). An almost linear speedup with the number of processors is observed and a 600×415 image is inverted in about 1 h using 32 processors (for detailed discussion see the separate publication by Spoelder[18]).

To test our method, the H_z field was calculated by means of Eq. (2) for a set of square wire frames in a plane, at equal spacing, and all carrying the same current. From this H_z field, using the method described above, we calculated the currents in the sample which should be equal to the chosen

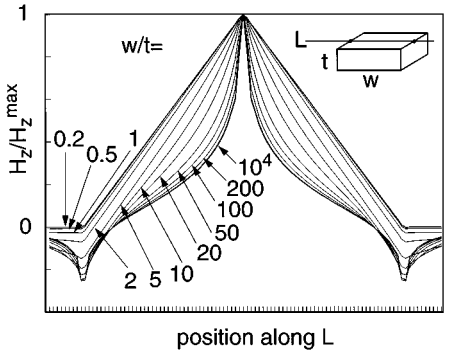

FIG. 4. Field profiles as a function of the sample's aspect ratio w/t, where w is the sample width and t is its thickness, as indicated in the inset. The profiles are taken along the line L (inset) on the surface of the sample. The sample is 81×81 pixels; the thickness is varied. All curves are normalized with respect to their maximum to clearly show the change in shape.

currents in the wire frames. In Figs. 3(d) and 3(e) the calculated current is shown along the line *a*-*a* through the center and parallel to a side of the square sample. The input current has the value 100. Clearly, within the bulk of the sample the currents are reproduced excellently. There is a small overestimation of the edge currents, but the deviation is limited to a band of a few pixels wide. In the center of the sample the current changes sign, which explains the dip in the center of the absolute current $|j|$ in Fig. 3(e): We cannot resolve currents on a scale smaller than one pixel. At this point we stress that our method is not only faster and more efficient in memory use than previous ones, but also more general: Equation (18) holds for samples of arbitrary thickness, while previous authors[9,10,17] considered infinitely thin samples. As will be seen below, this has the important advantage that it alleviates the problem of knowing exactly the distance between sample and detector (magneto-optical layer).

As a side result of the present work a method is found to calculate H_z from a known current distribution (and hence a known **g**) for a plane-parallel sample of arbitrary shape and thickness. For this purpose Eq. (18) is used without matrix inversion. As an example, the field H_z is calculated for a square sample of several thicknesses t but constant width w. The result for H_z at the surface of the sample and along the line through the center and parallel to a side is presented in Fig. 4. As expected, for thick samples with small aspect ratios w/t the triangular Bean profile is recovered, while for large aspect ratios the thin film result[1] is found. It is interesting to point out that even an aspect ratio $w/t\approx1$ (i.e., the sample is a cube) is large enough to yield almost the standard triangular Bean profile found in samples of infinite thickness (i.e., $w/t\rightarrow0$).

IV. ABSOLUTE CALIBRATION OF THE CURRENT DENSITY

As stipulated above, if the currents in the sample are to be determined not only relative to one another, but on an absolute scale (i.e., in A m^{-2}) there is a potential difficulty since the experimental configuration, in particular the sample-detector distance d, is often not known exactly. Of course, the distance from the sample can be determined quite accurately when d is large, but this is not useful since it leads to a great loss of detail in the observations. On the other hand, when the MO layer is placed directly on the sample, the effective distance from the sample is not known precisely. This is partly due to the surface roughness of sample and sensor and partly due to the thickness of the MO layer itself. To investigate the effect of the sample-detector distance d, the H_z field of a sample with aspect ratio 1/40 was calculated as a function of d. The result is shown in Fig. 5: The plot shows the value of the magnetic field on the fourfold symmetry axis of the sample as a function of distance d from the surface. The images 5(A)–5(H) show $|H_z|$ in the plane parallel to the sample surface at the distances indicated by the corresponding characters in the top graph. From the figure it is clear that for $d/t\gtrsim0.1$ the field is very much dependent upon distance, while for $d/t\ll0.1$ the field is constant. Clearly, quantitative measurements can easily be made if it is known that $d/t\ll0.1$; it is then not even necessary to know the value of d. Even for very thin single crystals this condition can be easily satisfied; for thin film samples, however, it may be more difficult. Incidentally, from the images in Fig. 5 it is clear that the magneto-optical images themselves indi-

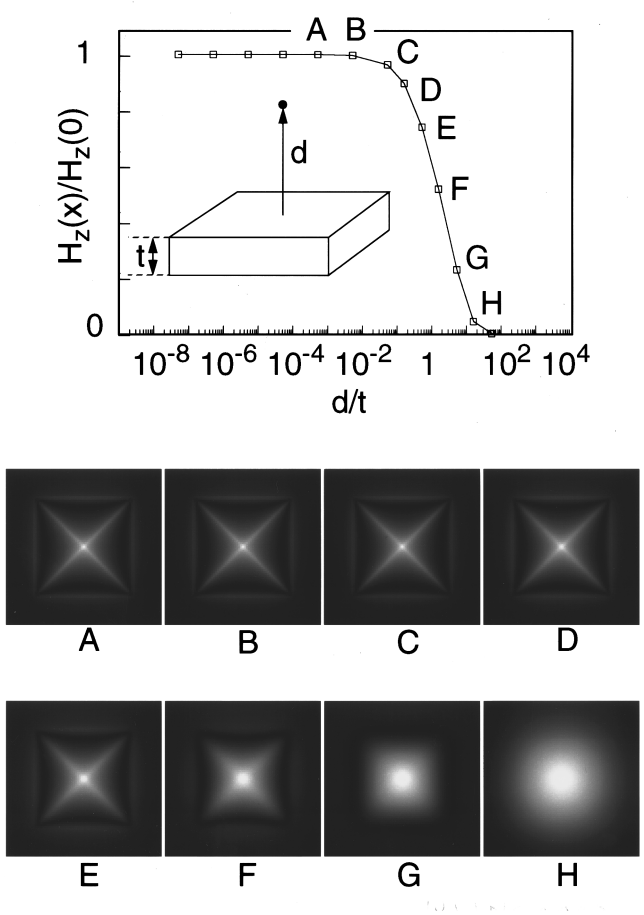

FIG. 5. Influence of the distance d between sample surface and detector plane on the magneto-optical image and H_z values. The graph shows H_z as a function of the ratio distance/thickness $(=d/t)$ on a line perpendicular to the sample and trough the center. The sample is 81×81 pixels with a thickness of 2 pixels; the distance is varied. The images, showing $|H_z|$ for selected distances, are also shown. If the distance is kept fixed and the thickness is varied, very similar (but not identical) results are found.

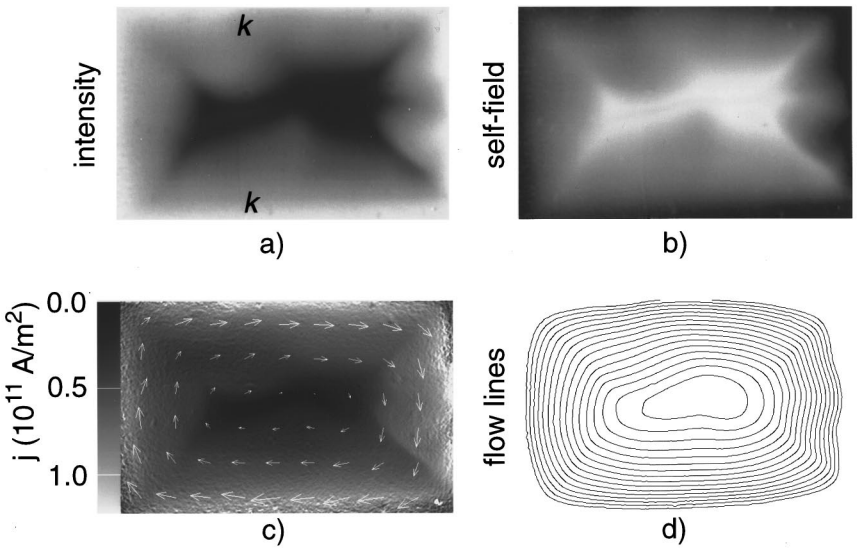

FIG. 6. Magneto-optical measurement on a $Bi_2Sr_2CaCu_2O_8$ crystal of $1.13\times0.67\times0.025$ mm^3. (a) Intensity image (the line kk is a scratch on the magneto-optical film), (b) the z component of the self-field, $H_z^{\rm self}$, and (c) the local currents as calculated from the algorithm discussed in the text. The grey scale indicates the absolute value of the current, and the arrows indicate the local current flow direction; the length of the arrows is proportional to $|j|$. (d) The contour lines of the g image, which are the current-flow lines.

cate whether or not the condition $d/t \ll 0.1$ applies: If not, then the image is blurred [images 5(E)–5(H)]. We note that our method of finding $\vec{j}(\vec{s})$ from $\vec{H}_z(x,y,d)$ only works so well because the sample thickness is taken into account explicitly in Eq. (16). This is a very important improvement over the older schemes.[9,10]

V. APPLICATION TO A REAL SAMPLE

To demonstrate the value of our inversion scheme, an experiment on a single crystal of the high-T_c superconductor $Bi_2Sr_2CaCu_2O_8$ was performed. Directly on top of the crystal a magneto-optical indicator was placed consisting of a glass substrate, an EuSe film of 250 nm, and an aluminum mirror layer of 100 nm thickness. This assembly was mounted in our home-built cryogenic polarization microscope[19] which is in the variable-temperature insert of an Oxford Instruments 7 T magnet system. The image is recorded by a low-light level CCD camera (Tokyo Electronic Industry CS8320C) connected to a videocassette recorder (Sony EVO-9650P). Images are grabbed and digitized using a Videopix frame grabber in a SUN workstation.

In the experiment the crystal was cooled in zero field from above its critical temperature down to 4.2 K. Subsequently the external field was raised to 2 T, which resulted in magnetic flux entering the superconductor and in shielding currents being established. As a consequence the local field is still zero in the center of the sample (there the self-field due to the shielding currents cancels the external field), while at its edges it is higher than the external field (the field of the shielding currents is parallel to the external field there).

In Fig. 6(a) the resulting magneto-optical image is shown. The vertical curved line kk is a scratch in the MO layer and is of no concern. The dark region in the center is the field-free region, while brighter regions correspond to higher local fields. From such an image first the local field $H_z^{\rm meas}$ is determined and then the self-field $H_z^{\rm self}$ is calculated as the difference of the local field and the applied external field $H_z^{\rm ext}$ see Eq. (1). From the self-field, the currents are determined using the algorithm described in the previous section. To find the local field from the magneto-optical intensity image, we first correct for possible uneven illumination. For this purpose a so-called illumination image of the sample is taken with uncrossed polarizers at a temperature above T_c. Ideally, under these circumstances the image should be uniform in intensity. After substraction of an offset of both images (necessary due to the electronics), any raw magneto-optical image [such as Fig. 6(a)] is divided by the illumination image to correct for uneven illumination.

To be able to determine the local field, a relation between intensity I and field H_z is needed. Since the Verdet constant can be field dependent, the functional dependence f in

$$I=\beta f(H_z^2) \tag{19}$$

is determined in a separate experiment for each MO layer and hence is known. The proportionality constant β depends among others upon the intensity of illumination. It can be found if the magnetic field at one position in the image is known. Generally, at large lateral distance from the sample the local field is equal to the known external field. Using the measured intensity at the same position, β can be found and hence Eq. (19) may be used to calculate the local field at any position in the image. During one experimental run the coefficient β is, in principle, the same for all images; hence the procedure just described can also be used for images in zero external field, where $f(H_z=0)=0$ and hence direct calibration is impossible. Depending on the camera used, sometimes β is slightly dependent upon the total intensity of the image. In such cases we use images at higher fields, but with the same total intensity to calibrate β for images around zero field. In this way, the local field is determined except for its sign, because the function f in Eq. (19) depends quadratically on H_z. In the actual magneto-optical experiments this sign, however, *can* be determined by rotating the analyzer since the Faraday effect results in a clockwise (anticlockwise) rotation of the polarization vector for positive (negative) fields. Mostly, however, the sign of the local field is known from the history of the experiment. In the example of Fig. 6(a), the local field has the same sign everywhere. By substraction of the external field from the local field one easily finds the self-field of the sample. In Fig. 6(b) the nega-

tive of the self-field is shown; i.e., black corresponds to zero self-field, while increasing brightness corresponds to increasingly negative values of the self-field. Using the procedure described in the previous section, the currents in the sample can be determined. Optionally the number of pixels may first be reduced to decrease the necessary calculation time; however, this also reduces the detail in the calculated current pattern. The result for 576×368 pixels (calculated using the IBM SP2/9076) is shown in Fig. 6(c). It is not our purpose to discuss the current pattern here. However, we note that the current is strongest along the edges of the sample and quickly falls off towards its center in agreement with calculations for thin samples.[1] The current vectors drawn on a rectangular grid in Fig. 6(c) easily yield a wrong visual impression of the current flow pattern. For this reason in Fig. 6(d) the contour lines of g, which are also the current-flow lines [see Eq. (3)], are shown.

The determination of local currents as described above is *quantitative*. The currents can be calculated with an estimated absolute accuracy of about 15%, mainly due to uncertainties in the calibration of the local field; the relative accuracy is, of course, much higher. To verify the calculation of the local currents, we also performed bulk magnetic moment measurements on the sample shown in Fig. 6(a), using a sensitive capacitance torque magnetometer.[20] If it is assumed that the current density j_s is uniform, a value $j_s=7\times10^{10}$ A m^{-2} is calculated from these measurements. This is indeed of the same order of magnitude as the currents determined magneto-optically and shown in Fig. 6(c), which have a maximum value around $j_s=1.2\times10^{11}$ A m^{-2}. Of course we know from Fig. 6(c) that the current distribution is not uniform. It is therefore not surprising that the average value determined from magnetic moment measurements is lower than the maximum local current.

VI. CONCLUSION

For a sample which is a rectangular cylinder of arbitrary cross section and arbitrary height, the currents flowing in it may be determined from magneto-optical measurements of the local H_z field, provided that the current vector has no z component. An fast algorithm with limited storage requirements and based on the conjugate gradient method was designed for this inversion and tested on a typical $Bi_2Sr_2CaCu_2O_8$ single crystal. The currents found from this algorithm agree well with those determined from bulk magnetometry. The same ideas can also be used for model calculations of the field generated by a 2D current pattern in plane-parallel arbitrarily shaped samples. With such simulations it is possible to calculate the magneto-optical image as a function of distance from the sample. By comparison with the experiment it is possible to estimate whether the detector layer is in close contact with the sample or not.

Although we have discussed only magneto-optical measurements of H_z, the method discussed in this paper is directly applicable to local-probe Hall measurements,[21] where an array of Hall probes is placed just above the sample and the local magnetic field is deduced from the Hall voltage in each individual sensor, since also with this method the local field can be measured at a large number of positions. With existing technology this number is, however, much small than the number of pixels in magneto-optical experiments.

Further improvements of the speed of the inversion algorithm might be found using a generalization of the Levinson algorithm for solving $\mathbf{a}=\mathbf{Mx}$, where $\mathbf{M}$ is a Toeplitz matrix.

The absolute accuracy of the magneto-optical method could be increased significantly if at (at least) one position the local field could be more accurately determined, e.g., by a Hall probe, while the spatial resolution of the Hall probe technique would benefit from combination with the magneto-optical one. Another possibility would be to measure simultaneously the magneto-optical response and the total magnetic moment of the sample. The experimental difficulties associated with such a combination are not small but worth the effort.

ACKNOWLEDGMENTS

We thank A.A. Menovsky and T.W. Li for the $Bi_2Sr_2CaCu_2O_8$ single crystal, J. Lankelma of Fokker Aircraft at Schiphol-Oost for drawing our attention to some properties of Toeplitz matrices, H.J. Boersma for discussions on Sec. II, and R. Bakker and G. Doornbos for help with the experiments. This work is part of the research program of the Stichting Fundamenteel Onderzoek der Materie (FOM), which is financially supported by the Nederlandse Organisatie voor Wetenschappelijk Onderzoek (NWO).

[1] E.H. Brandt, M.V. Indenbom, and A. Forkl, Europhys. Lett. **22**, 735 (1993).
[2] D.J. Frankel, J. Appl. Phys. **50**, 5402 (1979).
[3] E.H. Brandt, Physica C **235-240**, 2939 (1994).
[4] E. Zeldov, J.R. Clem, M. McElfresh, and M. Darwin, Phys. Rev. B **49**, 9802 (1994).
[5] Yu.A. Fedorov, V.G. Fleisher, and M.G. Semenchenko, Physica C **217**, 63 (1993).
[6] E.H. Brandt, Phys. Rev. Lett. **74**, 3025 (1995).
[7] H. Theuss, A. Forkl, and H. Kronmüller, Physica C **190**, 345 (1992).
[8] M.R. Koblischka, R.J. Wijngaarden, D.G. de Groot, R. Griessen, A.A. Menovsky, and T.W. Li, Physica C **249**, 339 (1995).
[9] E.H. Brandt, Phys. Rev. B **46**, 8628 (1992).
[10] W. Xing, B. Heinrich, H. Zhou, A.A. Fife, and A.R. Cragg, J. Appl. Phys. **76,** 4244 (1994).
[11] J.D. Jackson, *Classical Electrodynamics*, 2nd ed. (Wiley, New York, 1975), Eq. 5.14.
[12] J.D. Jackson, *Classical Electrodynamics*, 2nd ed. (Wiley, New York 1975), Eq. 5.56.
[13] L. Fruchter, A.P. Malozemoff, I.A. Campbell, J. Sanchez, J. Konczykowski, R. Griessen, and F. Holtzberg, Phys. Rev. B **43**, 8709 (1991).
[14] E.H. Brandt, Z. Phys. B **80**, 167 (1990).

[15] M.R. Koblischka and R.J. Wijngaarden, Supercond. Sci. Technol. **8**, 199 (1995), and references therein.
[16] Th. Schuster, M.R. Koblischka, H. Kuhn, B. Ludescher, M. Leghissa, M. Lippert, and H. Kronmueller, Physica C **196**, 373 (1992).
[17] See Sec. III C of Ref. 10.
[18] H.J.W. Spoelder (unpublished).
[19] R.J. Wijngaarden *et al.* (unpublished).
[20] H.G. Schnack, Ph.D. thesis, Vrije Universiteit Amsterdam, 1995; see also M. Qvarford, K. Heeck, J.G. Lensink, R.J. Wijngaarden, and R. Griessen, Rev. Sci. Instrum. **63,** 5726 (1992).
[21] Y.Abulafia, A. Shaulov, Y. Wolfus, R. Prozorov, L. Burlachkov, Y. Yeshurun, D. Majer, E. Zeldov, and V.M. Vinokur, Phys. Rev. Lett **75**, 2404 (1995).